

# Does CMIP5 Still Have Value Over CMIP6? A Case of Mean and Extreme Temperature Simulation Over Mainland India

Avijit Paul\* and Monomoy Goswami

Department of Civil Engineering, Central Institute of Technology Kokrajhar, Kokrajhar, Assam, India

Email: engr.avijit.paul@gmail.com (A.P.); monomoy99@hotmail.com (M.G.)

\*Corresponding author

Manuscript received September 15, 2023; revised November 1, 2023; accepted November 8, 2023; published April 15, 2024.

**Abstract**—Observations about inadequacy of General Climate Models (GCMs) of the sixth phase of Climate Model Intercomparison Project (CMIP6) in simulating different climatological variables in several regions of the world prompted the examination of the performance of GCMs of the preceding fifth phase (CMIP5) phase vis-à-vis those of CMIP6 in simulating mean and extreme temperatures over a physiographically diverse mainland India. Selected statistics of daily temperature, simulated at 0.25×0.25 grid by 30 GCMs of CMIP6 and 28 of CMIP5, were compared with those of reference data of 27 years for performance assessment of the two phases. Significance Score, Mean Absolute Error and Index of Agreement, were applied to explore the spatial distribution of the best-performing model of each CMIP phase, and an innovative rank-based approach was devised and Taylor diagrams were used to examine the spatially aggregated performance of the models. GCMs of both CMIP6 and CMIP5 were found as being valuable in simulating one or the other temperature statistic in one or the other part of the country with no indication of one phase being consistently better than the other. The results of this extensive study shows that, the focus of development of each CMIP phase being unique, a model of CMIP5 could also have the potential of outperforming the models of CMIP6 in simulating climate variables, and that, in the case of mainland India, a GCM of either of the two phases would be appropriate for reliable projection of location-specific future temperature under different climate change scenarios.

**Keywords**—Coupled Model Intercomparison Project Phase 5 (CMIP5), Coupled Model Intercomparison Project Phase 6 (CMIP6), General Climate Model (GCM), temperature, simulation, India

## I. INTRODUCTION

A changing climate impacts a region's hydrometeorological phenomena, water resources, agriculture, energy, human health and other ecologically and socio-economically relevant sectors [1–15]. India is a large and populous region of the world with its physiographical and hydrometeorological diversities influencing the spatiotemporal pattern of occurrence of climatological variables across the country's vast expanse rendering the country vulnerable to impacts of climate change [16–18]. Reducing the vulnerabilities by offsetting the detrimental impacts of climate change through adaptation and mitigation requires the understanding of the state of climate, the reliable projection of the future climate, and a scientific assessment of the likely impacts of the change. The extensivity of climate, the variability of its components, the complexity of component-interactions and the current state of technological development make it compelling to have recourse to climate models to meet the above requirements.

The Coupled Model Intercomparison Project (CMIP) under the World Climate Research Programme (WCRP)

provides outputs from an extensive collection of coupled climate and Earth System models, and aims at understanding the “past, present and future climate changes arising from natural, unforced variability or in response to changes in radiative forcing in a multi-model context” [19]. Beginning in the year 2013, Coupled Model Intercomparison Project Phase 6 (CMIP6) is the latest phase of development of the CMIP project [20] that, according to WCRP-CMIP CMIP6\_CVs version: 6.2.58.54 [21], has participations from modelling groups from 49 Institutions across the world, and includes 132 General Climate Models (GCMs) released over the period from 1989 to 2022. CMIP6 provided global climate model data assessed in the Sixth Assessment Report of the Intergovernmental Panel on Climate Change (IPCC) [22, 23]. The preceding fifth phase of the CMIP, i.e., CMIP5, during the period from 2010 to 2014 included more than 50 GCMs, and served as a basis for the IPCC's Fifth Assessment Report [24, 25]. Whereas CMIP5 explored earth system processes, such as, carbon cycle, aerosol, biogeochemistry, dynamical vegetation components, cloud feedback, etc. through long-term and short-term integration experiments [24, 26, 27], CMIP6 aimed at exploring the earth system's response to forcing, the origins and consequences of systematic model biases, and the future changes in climate under internal climate variability, predictability and uncertainties in scenarios [20, 28]. However, because of the focus of development of the two phases being different, it emerged from several studies of comparison of the models of CMIP6 and CMIP5 applied either individually or as Multi Model Ensembles (MMEs) across countries and regions of the world that the CMIP6 models did not perform consistently better than the CMIP5 models in climate simulation. In simulating extreme daily temperature and precipitation across the global landmass, Li *et al.* [29] did not find advantage of CMIP6 models over CMIP5 models in simulating total precipitation and continuous dry days, and observed that, except for continuous dry days, the uncertainty estimation by CMIP6 models in simulating total precipitation and very wet days were larger than those by CMIP5 models; Wehner *et al.* [30] found that, individually, no CMIP5 or CMIP6 model could be identified as being distinctly superior; Fan *et al.* [31] reported improved performance of some individual CMIP6 models in simulating spatial pattern of summer days, tropical nights, cold spell duration, and diurnal temperature range amongst 16 indices of temperature extremes relative to CMIP5 models and relatively unsatisfactory performance of the MMEs of the both phases in simulating the spatial patterns of duration and percentile indices; Chen *et al.* [32] noted a general improvement of

CMIP6 models in simulating temperature and precipitation extremes and their trend patterns compared to observations, but a limited or even decreased improvement in regard to the spread of some individual CMIP6 models in comparison with their predecessors; and Kim *et al.* [33] concluded that CMIP6 models generally captured the patterns of temperature extremes with limited improvements in comparison with their CMIP5 counterparts, amongst others.

In regard to assessing the relative performance of different CMIP phases for simulating climate variables over India's landmass, studies of relative performance of CMIP6 and CMIP5 Models are rather limited, and the scenario of studies with models of the previous CMIP phases is no better (e.g., [34] and [35] on comparison of models of CMIP5 and those of the third phase of the CMIP, i.e., CMIP3; [36–40] on application of models of CMIP6 phase alone; and [35, 36, 41–44] on the use of individual GCMs of the pre-CMIP6 phases). This sparsity of studies of India's climate, although an integral and important component of the global climate system, is generally attributable to the sparsity of good quality data of relatively high spatiotemporal resolution over reasonably long periods of time, and inaccuracy of estimation of the climate sub types across the diverse topography of India by climate models [35, 40]. In regard to the comparison of CMIP6 and CMIP5 models applied to climate variables over India, Gusain *et al.* [44] found by using APHRODITE (Asian Precipitation - Highly-Resolved Observational Data Integration Towards Evaluation of Water Resources) for observational data that the spatial improvement of CMIP6 models over CMIP5 models in simulating Indian Summer Monsoon Rainfall (ISMR) was inconsistent. Salunke *et al.* [45] found that CMIP6 Multi Model Means performed better than the CMIP5 counterparts in simulating spatial distribution of seasonal mean precipitation and in capturing precipitation trends, but could not simulate the overall decreasing trend in the observed data of India Meteorological Department (IMD). Dutta *et al.* [46] analyzed the global teleconnections of the Indian Summer Monsoon clouds using CMIP6 and CMIP5 MMEs and found improvement in seasonal mean bias of total cloud fraction and rainfall over the Asian Summer Monsoon Region from CMIP5-MME to CMIP6-MME. Sreekala *et al.* [47] found poor skill of the models of CMIP6 and CMIP5 and of the respective MMEs in simulating northeast monsoon rain over southern peninsular India.

Conspicuously, most of the studies of the state of climate and climate change impacts over India focus on the relative performance of GCMs in simulating different aspects of the ISMR. This is not surprising because of more than 80% of the country's annual precipitation necessary for the sustenance of its population of more than one fifth of that of the world being derived from the ISMR, and the country's seasonal rainfall being highly crucial for its agriculture and many other facets of life [40, 48]. However, temperature being an influencer of climate systems, an important variable of all fields of natural science, and an indicator of global warming and associated climate change, the need to study different aspects of temperature is also highly important. Accordingly, the objective of this study was set to explore the applicability of GCMs of CMIP6 and CMIP5 in simulating the mean, maximum and minimum temperatures and their extremes

across mainland India (excluding the islands) at spatiotemporal resolutions of  $0.25^\circ \times 0.25^\circ$  grids and comparing the relative performance of the two CMIP phases.

For comparing performance of different GCMs, historical series of observed data of selected variables are required at high spatial and temporal resolutions. In the case of India, the India Meteorological Department (IMD) provides observational data of maximum and minimum temperature in  $1.0^\circ \times 1.0^\circ$  grids covering the entire country at daily timesteps [49]. However, in order to avail reference data at a finer spatial resolution of  $0.25^\circ \times 0.25^\circ$  grid, reanalysis data that assimilate multiple observational data of the atmosphere, land and ocean into a forecast model yielding a 'dynamically consistent estimate' of the state of climate at different timesteps [50] was considered as being substitutes of observational data. Accordingly, noting from an earlier study by [51] that reanalysis data of the European Centre for Medium-Range Weather Forecasts (ECMWF) of the fifth generation, i.e. ECMWF Re-Analysis 5 (ERA5), performed better amongst five reanalysis datasets in representing monsoon precipitation, maximum temperature, evapotranspiration and soil moisture over India, ERA5 data of surface temperature were adopted in this study as reference data for meeting the objectives of this study.

In order to assess the performance of climate simulation models, several stand-alone indices and composite measures were considered by researchers. Each of these criteria assesses either the probabilistic or the deterministic or the trend characteristics of the series of data being simulated. The choice of suitable criteria for a study depends on the interpretability of these criteria in matching the objective(s) of the study. In this study, the Significance Score [41, 52–59] based on Probability Density Function (PDF), the residual-based Mean Absolute Error and Index of Agreement [35, 60–65], and the multi-measure-based Taylor diagram [27, 30, 62, 66–75] were used, and an innovative rank-based approach was devised for evaluating the performance of different climate models in representing both probabilistic and deterministic aspects of temperature.

## II. STUDY AREA AND DATA

This study covers the mainland India (excluding islands) lying between  $8^\circ 4'$  and  $37^\circ 6'$  North latitude and  $68^\circ 7'$  and  $97^\circ 25'$  East longitudes, and bounded by the Bay of Bengal, the Arabian Sea and the Indian Ocean on the south and the Himalayas Mountain ranges on the north. The elevation of the land ranges from mean sea level to more than 8200 meter as shown in Fig. 1(a), and comprises mountains and hills, riverine plains, coastal areas and desert. Climatologically the land is divided into five zones, namely hot-dry, warm-humid, composite, temperate and cold as exhibited in Fig. 1(b) by following the National Building Code of India [76]. The geographic, topographic, and climatic diversities necessitated the mainland India to be divided into six hydrometeorologically homogeneous zones and 25 subzones (excluding the Andaman and Nicobar Island which is considered as being the seventh zone and the 26<sup>th</sup> subzone) as described in the Flood Estimation Reports by the Central Water Commission (CWC), e.g., [77], of India and other literatures, e.g., [78]. A total of 4964 grid points at  $0.25^\circ \times 0.25^\circ$  grids covers the mainland India, and are

considered for this study. The long-term average temporal variation of daily maximum temperature ( $T_{max}$ ), daily mean temperature ( $T_{mean}$ ) and daily minimum temperature ( $T_{min}$ ) aggregated month-wise across these grid points in degree Celsius ( $^{\circ}\text{C}$ ) unit over the period from 1979 to 2005, and the box and whisker plot showing the range, dispersion and skewness of the spatially distributed temperature variables are presented in Fig. 1(c) and 1(d) respectively. Whereas the temporal variation shows seasonality of temperature with the peak occurring in the month of May preceding the onset of ISMR and the minimum occurring in January, the box-and-whisker plot shows a large variation of temperature across the country, obviously imposing challenge to GCMs in

simulating the past temperature.

For the study, temperature outputs from GCMs of CMIP6 and CMIP5 were sourced from the data portals of WCRP hosted by Lawrence Livermore National Laboratory of the US Department of Energy, and GCMs were selected based on the concurrent availability of the three temperature variables  $T_{max}$ ,  $T_{mean}$  and  $T_{min}$  as outputs of the GCMs. Accordingly, temperature outputs of 30 GCMs of CMIP6 and 28 of CMIP5 were downloaded in NetCDF format for a 27-year period from 1979 to 2005 for further processing. The details of the selected GCMs of CMIP5 and CMIP6 are provided in Annexures A-1 and A-2 respectively.

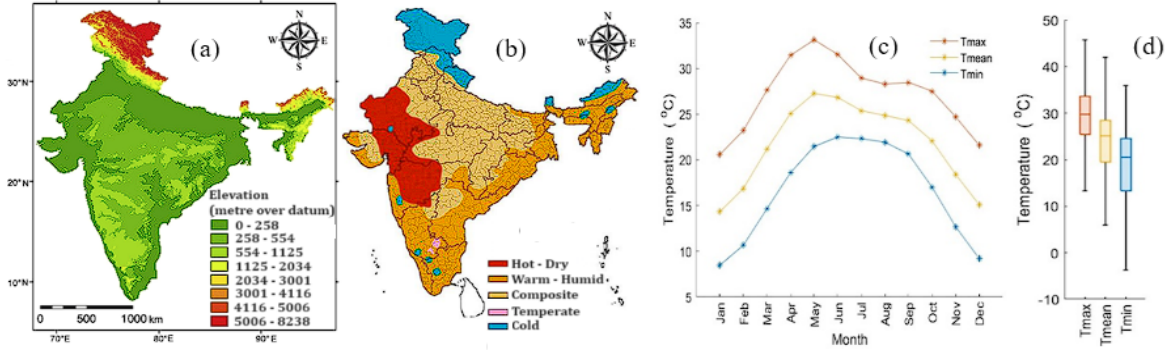


Fig. 1. Topographic and climatic characteristics of mainland India (a) Elevation (b) Climatic zones (as per National Building Code, 2016) (c) Monthly variation of  $T_{max}$ ,  $T_{mean}$  and  $T_{min}$  and (d) Range of variation of  $T_{max}$ ,  $T_{mean}$  and  $T_{min}$ .

For simulation, the reference data of  $T_{max}$ ,  $T_{mean}$  and  $T_{min}$  for concurrent period are obtained in degree Kelvin unit (k) and converted to Celsius  $^{\circ}\text{C}$  from ‘2m temperature’ hourly data at  $0.25^{\circ}\times 0.25^{\circ}$  grids from the ERA5 dataset available at the Copernicus Climate Change Service Climate Data Store of the ECMWF). These data provide air temperature at 2 m above the surface of land, and are stated as being produced by combining ‘vast amounts of historical observations into global estimates using advanced modelling and data assimilation systems’ ‘into a globally complete and consistent dataset using the laws of physics’ [79].

### III. METHODOLOGY

The GCM-simulated data were re-gridded to  $0.25^{\circ}\times 0.25^{\circ}$  coordinates using Climate Data Operators (CDO) software tool [80]. For the series of reference data at each grid point of the  $0.25^{\circ}\times 0.25^{\circ}$  grids, the daily maximum and minimum temperatures were derived from the hourly data of each day, and the daily mean temperature was computed by taking average of the 24-h values of a day.

After data processing, the simulation-performance of each of the CMIP6 and CMIP5 models across mainland India was assessed by adopting three approaches. In the first approach, the degree of match of the PDFs, the degree of temporal correspondence and the conservation of descriptive statistics of the reference and GCM-simulated data were examined by separately considering data on annual, i.e., whole-year, basis, and on the basis of four seasons of three months each, i.e., monsoon or summer (JJA), post-monsoon (SON), winter (DJF) and pre-monsoon (MAM) by representing each month by the first letter of its name. For comparing the PDFs, the Significance Score ( $S_{Score}$ ) given by equation (1) was used.

$$S_{Score} = \sum_1^M \text{minimum}(Z_s, Z_r) \quad (1)$$

Here  $M$  is the number of bins used to calculate the PDFs, and  $Z_s$  and  $Z_r$  are the frequencies in a given bin of the GCM-simulated and reference data respectively. As suggested by [52] for temperature variables, a bin size of  $0.5^{\circ}\text{C}$  is adopted. The value of this score equal to 1 implies a perfect simulation.

For assessing the simulation performance of deterministic characteristics, the Mean Absolute Error ( $MAE$ ) and Index of Agreement ( $IoA$ ) given by equations (2) and (3) were adopted.

$$MAE = \frac{1}{N} \sum_1^N |y_i - r_i| \quad (2)$$

$$IoA = 1 - \frac{\sum_1^N (y_i - r_i)^2}{\sum_1^N (|y_i - \bar{r}_i| + |r_i - \bar{r}_i|)^2} \quad (3)$$

where  $y_i$  and  $r_i$  are the GCM-simulated and reference data of the  $i^{\text{th}}$  day, and  $\bar{r}_i$  and  $N$  are the mean and the number of reference data respectively at each grid point. Here  $MAE$  provides a measure of average error between simulated and reference data and  $IoA$  yields a measure of average error relative to a combination of the systematic and the unsystematic components of the average error set in the format of variance. Whereas the  $MAE$  is dimensioned with no upper bound, the  $IoA$  is dimensionless and bounded by 0 and 1. A smaller value of  $MAE$  and a larger value close to unity of  $IoA$  indicate a better representation of the deterministic characteristics of a variable by a model.

Based on the values of  $S_{Score}$ ,  $MAE$  and  $IoA$  applied to the series of annual data of 27 years for each temperature variable at each grid point, the 58 GCMs of both CMIP phases were ranked by separately assigning rank 1 to the GCM attaining the highest values of  $S_{Score}$  and  $IoA$  and the

lowest value of *MAE*. From the highest rank, i.e., rank 1, of the GCM, the CMIP phase associated with that GCM could be identified for each measure of performance at each grid point, the spatial distribution of the better-performing CMIP phase was explored. After the consideration of annual data, the seasonal values of temperature were likewise considered to explore season-wise performance of simulation by the GCMs.

Subsequently, for exploring the spatially averaged performance over the study area by considering annual data, the values of *S<sub>Score</sub>*, *MAE* and *IoA* were individually averaged across all grid points for each GCM from which the GCMs were ranked for each measure for each temperature variable. The performance of the GCMs based on an overall performance for each temperature variable was then explored by adding the three equally-weighted ranks of each GCM obtained from *S<sub>Score</sub>*, *MAE* and *IoA*, thereby creating a ranked list of the GCMs based on the combined rank having  $3 \times 1 (=3)$  and  $58 \times 3 (=174)$  as the smallest and the highest possible values respectively. From this list, the spatially averaged performance of the GCMs and the corresponding CMIP phase for each of the *T<sub>max</sub>*, *T<sub>mean</sub>* and *T<sub>min</sub>* variables over mainland India was assessed.

For exploring the performance of the GCMs in simulating the whole range of temperature over mainland India, the ranks of the GCMs in the ranked list obtained in the preceding step were further aggregated by adding the values of the ranks of each GCM for each of the *T<sub>max</sub>*, *T<sub>mean</sub>* and *T<sub>min</sub>* variables. A final ranked list having  $3 \times 3 (=9)$  and  $174 \times 3 (=522)$  as the smallest and the highest possible values respectively was thereby obtained. The ranks thus innovatively devised facilitated a broad assessment of the spatially-averaged performance of the GCMs and the corresponding CMIP phase in simulating the whole range of temperature across mainland India, and facilitated the identification of the best GCM of each CMIP phase based on spatial averaging for further study.

In the second approach, the performance in terms of spatial similarity of the GCMs of the two CMIP phases in simulating the reference data at all grid points across the mainland India was assessed for each temperature variable by pooling, i.e., spatially aggregating, the data of all grid points in a single series. Taylor diagrams were produced by evaluating and plotting the Correlation Coefficient (CC), centered Root Mean Square Error (RMSE) and Spatial Standard Deviation (SSD) between the reference data and the data simulated by each GCM by considering annual and seasonal data over the study area.

Whereas the above two approaches reveal the performances of the GCMs across the range of each temperature variable from annual or seasonal considerations, the ability of the GCMs in simulating the extremes is also important. Accordingly, a third approach was adopted whereby the percent over- and under-estimation of the 1<sup>st</sup> and 99<sup>th</sup> percentiles of the reference data at the grid points across mainland India by each GCM were explored for each temperature variable by considering annual data. The over- and under-estimations of the two selected percentiles by the best GCM of each CMIP phase as identified from spatial averaging in the first approach of methodology were also evaluated at the grid points of mainland India, and maps were

produced to investigate the performance of the models of the two CMIP phases.

#### IV. RESULT AND DISCUSSION

##### A. Spatial Distribution of Performance of CMIP6 and CMIP5 Models

The spatial distribution of the best-performing CMIP phase as identified in the first approach based on each of the three measures of performance, namely *S<sub>Score</sub>*, *MAE* and *IoA*, for each of the three temperature variables, namely *T<sub>max</sub>*, *T<sub>mean</sub>* and *T<sub>min</sub>*, by separately considering annual and seasonal data across mainland India are exhibited in Figs. 2–4. It may be seen from these figures that, the spatial coverage as assessed in %age of grid points covering mainland India in simulating *T<sub>max</sub>* on the basis of annual data works out as being higher by the models of CMIP6 than those of CMIP5 for all three measures of performance. A similar observation is made for the models of CMIP6 when data of the summer season (JJA) is considered for simulation of *T<sub>max</sub>*. This appears as being obvious because the maximum temperature of a year is expected to occur in summer. In contrast, the spatial coverage of the models of CMIP5 emerges as being generally higher than those of CMIP6 in simulating *T<sub>mean</sub>* and *T<sub>min</sub>* on the basis of annual data when evaluated with *MAE* and *IoA*, and at par in simulating *T<sub>min</sub>* when evaluated with *S<sub>Score</sub>*. The higher spatial coverage of the models of CMIP5 is also found in simulating *T<sub>mean</sub>* in winter (DJF) when evaluated with all three measures of performance and in pre-monsoon (MAM) when evaluated with *MAE* and *IoA*, and in simulating *T<sub>min</sub>* in winter when evaluated with *MAE*, in pre-monsoon when evaluated with *IoA*, and in summer when evaluated with *S<sub>Score</sub>*. For the post-monsoon season, the spatial coverage by the models of CMIP6 appears as being consistently higher than those of CMIP5 for simulating all three temperature variables. From the above it is concluded that, although, in line with the expectation of higher performance by models of a latest phase of development, the best-ranking models of CMIP6 perform with a higher spatial coverage in simulating *T<sub>max</sub>* when evaluated with annual data and the data of summer and post-monsoon seasons, the models of CMIP5 outperform those of CMIP6 in simulating *T<sub>mean</sub>* and *T<sub>min</sub>* on the basis of annual data and with data of several seasons. These results show that the GCMs of CMIP5 still have value in reproducing the maximum, mean and minimum temperature at locations across mainland India based on their geographic disposition, and the temperature statistic and the annual or seasonal data considered, and, hence, in future projections of climate impacts.

Another finding of the spatial distribution of best performing models of the two CMIP phases is a possible correspondence of the spatial pattern of the distribution with the topographical and climatological features of mainland India. In comparison with Fig. 1, it appears from Figs. 2–4 that, for simulation of *T<sub>max</sub>*, the GCMs of CMIP6 generally perform better in flat and low altitude areas of the west and central India, and in high-altitude areas of the north, northeast and south India that are characterized by hot-dry, temperate and warm-humid climatic zones. Similarly, for simulation of *T<sub>min</sub>*, the GCMs of CMIP5 generally perform better in the alluvial flood plains of the north and northeast India and

high-altitude areas of the south and east India that are characterized by cold, composite and warm-humid climatic zones. Correspondence of  $T_{mean}$  simulated by CMIP6 models with topographical and climatological features, although

likely in the hot-dry western region of the country with  $S_{Score}$  and  $MAE$  as measures of performance, is not obvious when  $IoA$  is used as the measure of model performance.

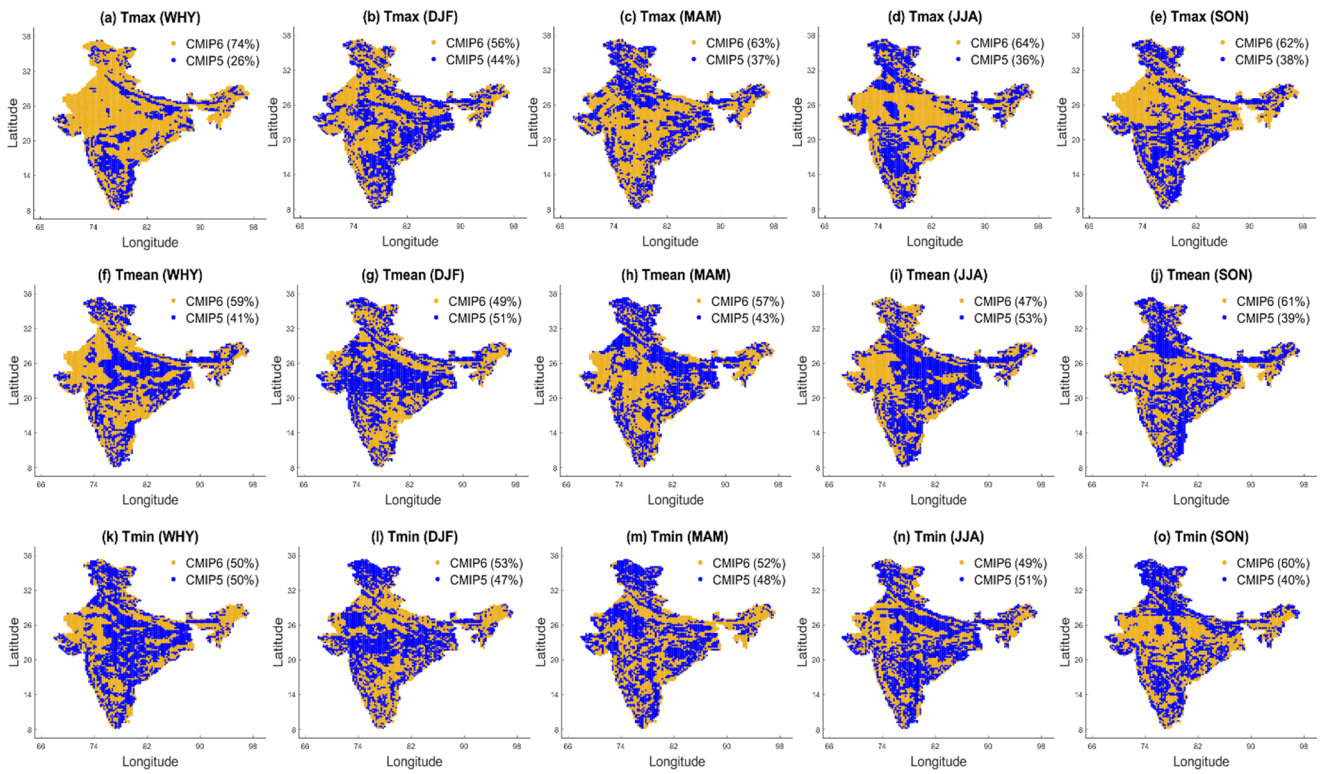


Fig. 2. Spatial distribution of CMIP6 and CMIP5 models based on the highest  $S_{Score}$  considering data of whole year (WHY) and four seasons (DJF, MAM, JJA, SON) in (a)-(e) for  $T_{max}$ , (f)-(j) for  $T_{mean}$ , and (k)-(o) for  $T_{min}$ .

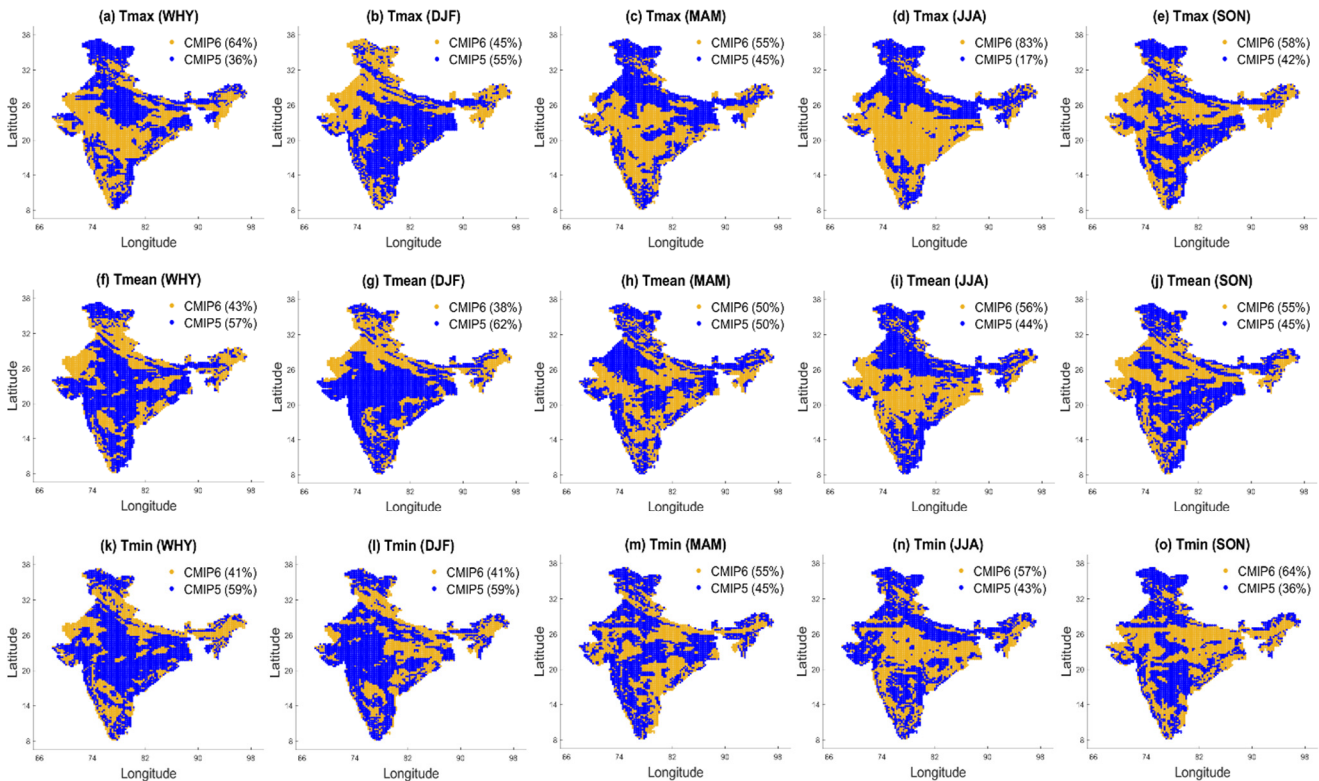


Fig. 3. Spatial distribution of CMIP6 and CMIP5 models based on the least  $MAE$  considering data of whole year (WHY) and four seasons (DJF, MAM, JJA, SON) in (a)-(e) for  $T_{max}$ , (f)-(j) for  $T_{mean}$ , and (k)-(o) for  $T_{min}$ .

### B. Spatially Averaged Performance of CMIP6 and CMIP5 Models

On application of spatial averaging, the ranks attained by

the models of the two CMIP phases in simulating  $T_{max}$ ,  $T_{mean}$  and  $T_{min}$  are presented in Fig. 5, and those obtained on combination of the ranks for  $T_{max}$ ,  $T_{mean}$  and  $T_{min}$  from the

consideration of simulating the whole range of temperature over the study area are exhibited in Fig. 6. In these figures, a smaller value of a rank indicates a better performing model. It may be observed from Fig. 5 that, overall, for mainland India, EC-Earth3 and EC-Earth3-Veg of CMIP6 are the best performing GCMs for simulating  $T_{max}$  and  $T_{mean}$  respectively, and ACCESS1-0 of CMIP5 is the best performing GCM for simulating  $T_{min}$ . Fig. 5 also shows that, between the best and the worst ranks, the models of the two CMIP phases are fairly scattered with no indication of the models of any one phase being consistently better than those of the other. On aggregation of the ranks of each model in simulating each of  $T_{max}$ ,  $T_{mean}$  and  $T_{min}$ , the aggregated ranks of 58 models are presented in Fig. 6. It may be seen from this figure that the GCMs named EC-Earth3 and EC-Earth3-Veg of CMIP6 and CMCC-CMS of CMIP5 appear as being the best, second-best and third-best models respectively. In this analysis, the performances of the second- and third-best models from CMIP6 and CMIP5 respectively emerged as being very close.

The above observations substantiate the earlier findings regarding the value of CMIP5 as also of CMIP6. As an outcome of this analysis, EC-Earth3 of CMIP6 and CMCC-CMS of CMIP5 were considered for further analysis of temperature with the best model from each CMIP phase. In order to explore the applicability of the generally high performing EC-Earth3 model of CMIP6 and CMCC-CMS model of CMIP5 for simulating  $T_{max}$ ,  $T_{mean}$  and  $T_{min}$  at all grid points of mainland India, the values of the three measures of performance produced by these two models are presented on the map of India in Figs. 7 and 8. It may be seen from these figures that the pattern of performance in simulating the three temperature variables over mainland India by the GCM of CMIP6 is generally comparable to that of CMIP5 for each of the three measures of performance with both models performing relatively poorly in the north, northeast and western coastal regions of India. This observation implies that any of these two models, one from each CMIP phase.

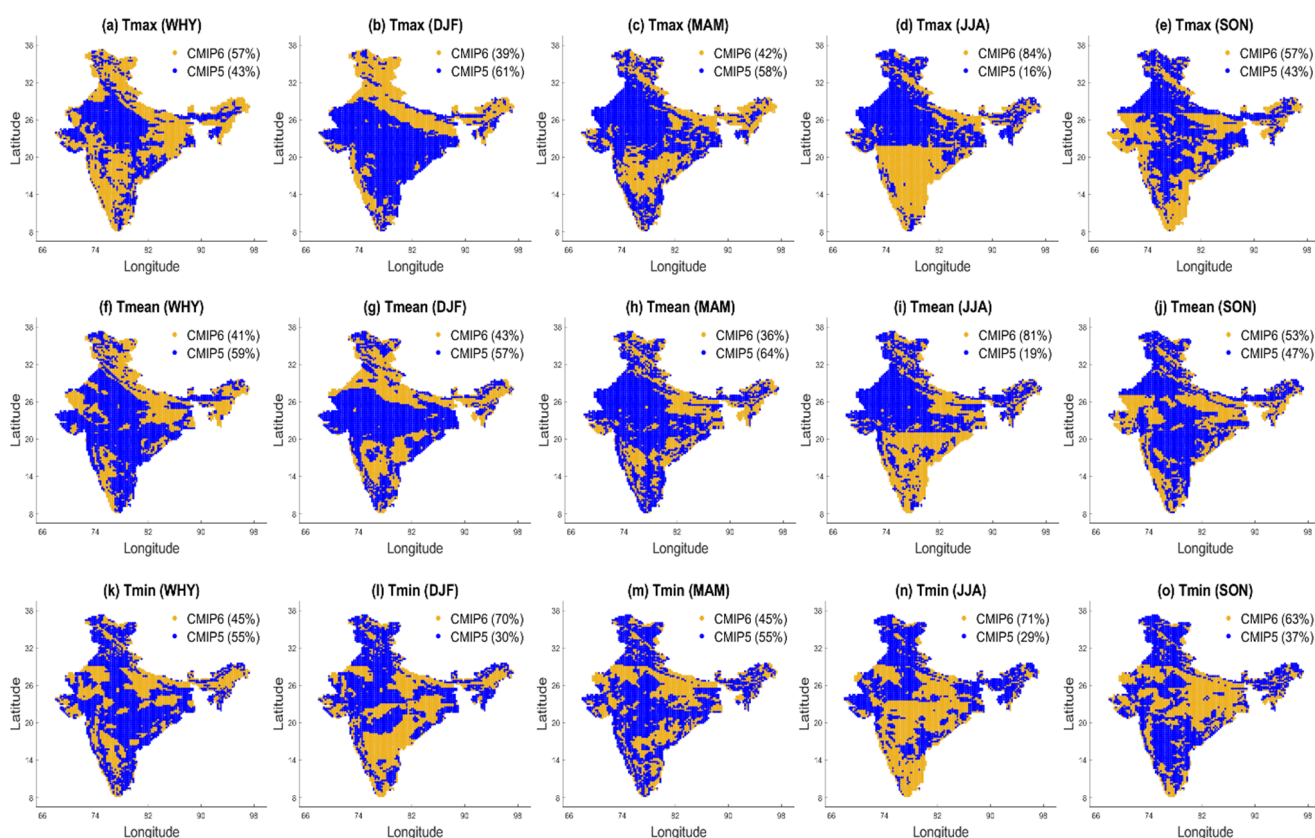


Fig. 4. Spatial distribution of CMIP6 and CMIP5 models based on the highest  $IoA$  considering data of whole year (WHY) and four seasons (DJF, MAM, JJA, SON) in (a)-(e) for  $T_{max}$ , (f)-(j) for  $T_{mean}$ , and (k)-(o) for  $T_{min}$ .

### C. Spatial Similarity of Performance of CMIP6 and CMIP5 Models

The Taylor diagrams produced for  $T_{max}$ ,  $T_{mean}$  and  $T_{min}$  by following the second approach of aggregating, i.e., pooling the data of all grid points, by considering the annual and seasonal data are presented in Fig. 9. The Taylor diagrams in this figure do not exhibit any distinct clustering of models of different CMIP phases or a large scatter of the models. The models in all tests of simulating the three temperature variables are found to be closely spaced within the 0.8 to 0.95 band of CC with most tests showing the models achieving the values of CC between 0.9 and 0.95. Most models are also found to lie within the 4 to 6°C band of the centered pattern

RMSE. The values of SSD of the models in the tests with annual data are found to be generally evenly distributed around and relatively less deviated from that of the reference data, whereas those for the tests with seasonal data show relatively more deviations from the SSD of the reference data with several tests showing models with SSD less than that of the reference data. However, the distribution of the models of CMIP6 and CMIP5 indicated respectively by blue and red colours on the Taylor diagrams do not suggest that the performance of the models of one CMIP phase would be better than that of the other; rather, some models of both phases are found to lie on the red arc representing the SSD of the reference data on the Taylor diagrams with comparable

values of CC and centered pattern RMSE. Overall, the above observations reinforce the earlier findings that the GCMs of CMIP5 also have value, and are likely to produce reliable

estimates of temperature variables in reproducing historical data and projecting future occurrences.

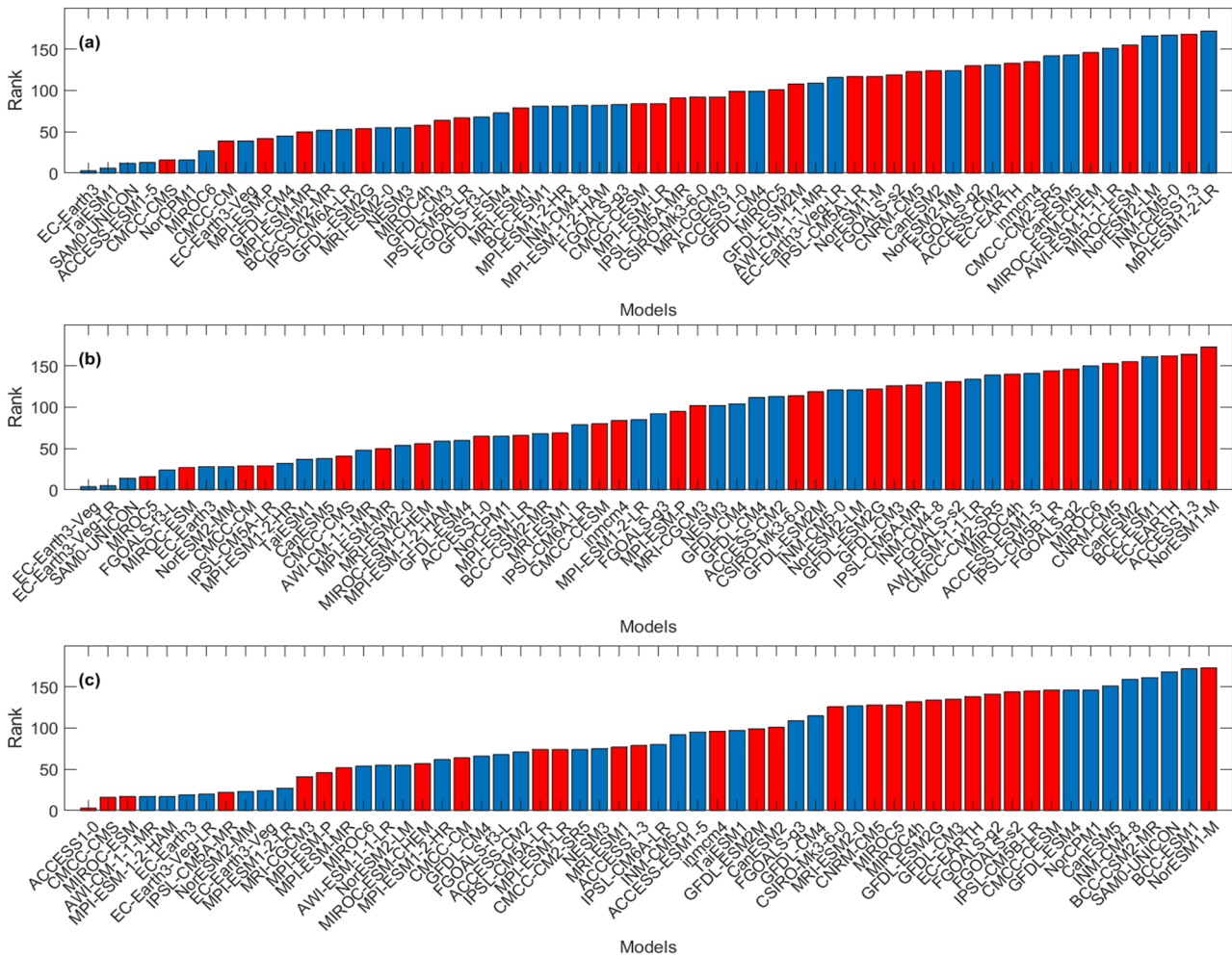


Fig. 5. Spatially averaged ranks of GCMs of CMIP6 (blue) & CMIP5 (red) in simulating (a)  $T_{max}$ , (b)  $T_{mean}$  and (c)  $T_{min}$ .

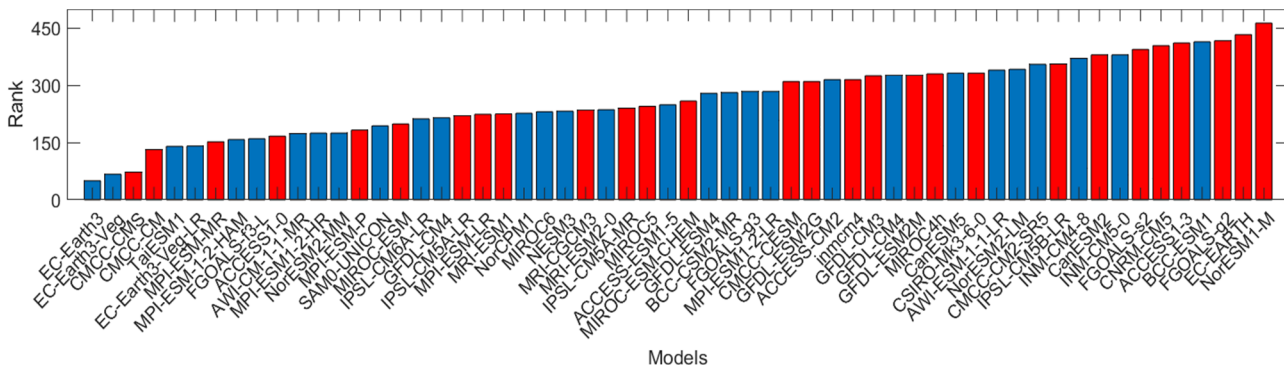


Fig. 6. Spatially averaged ranks of GCMs of CMIP6 (blue) & CMIP5 (red) obtained by aggregating the ranks for  $T_{max}$ ,  $T_{mean}$  and  $T_{min}$ .

**D. Performance of CMIP6 and CMIP5 Models in Simulating Temperature Extremes**

In investigating the performance of the two CMIP phases in simulating temperature extremes, the underestimations occurring in percentage of grid points in simulating the 1<sup>st</sup> and 99<sup>th</sup> percentile of each of the three temperature variables  $T_{max}$ ,  $T_{mean}$  and  $T_{min}$  over the whole data period by the models of the two CMIP phases are graphically presented in Fig. 10. It may be seen from this figure that the percentage of grid points for which the 1<sup>st</sup> percentile of each variable is underestimated is relatively less for all models, thereby

implying that the upper extremes of the reference data are either overestimated or reproduced at par on simulation by the GCMs of the both CMIP phases at most of the grid points. In contrast, underestimations occur in simulating the 99<sup>th</sup> percentile of the reference data in a large percentage of grid points for all three temperature variables with a small fraction of grid-points associated with over- or at par estimation. However, all models of the both CMIP phases are found to yield comparable percentages of over- or under-estimations with no distinct display to differentiate the models of one CMIP phase as being better than those of the other.

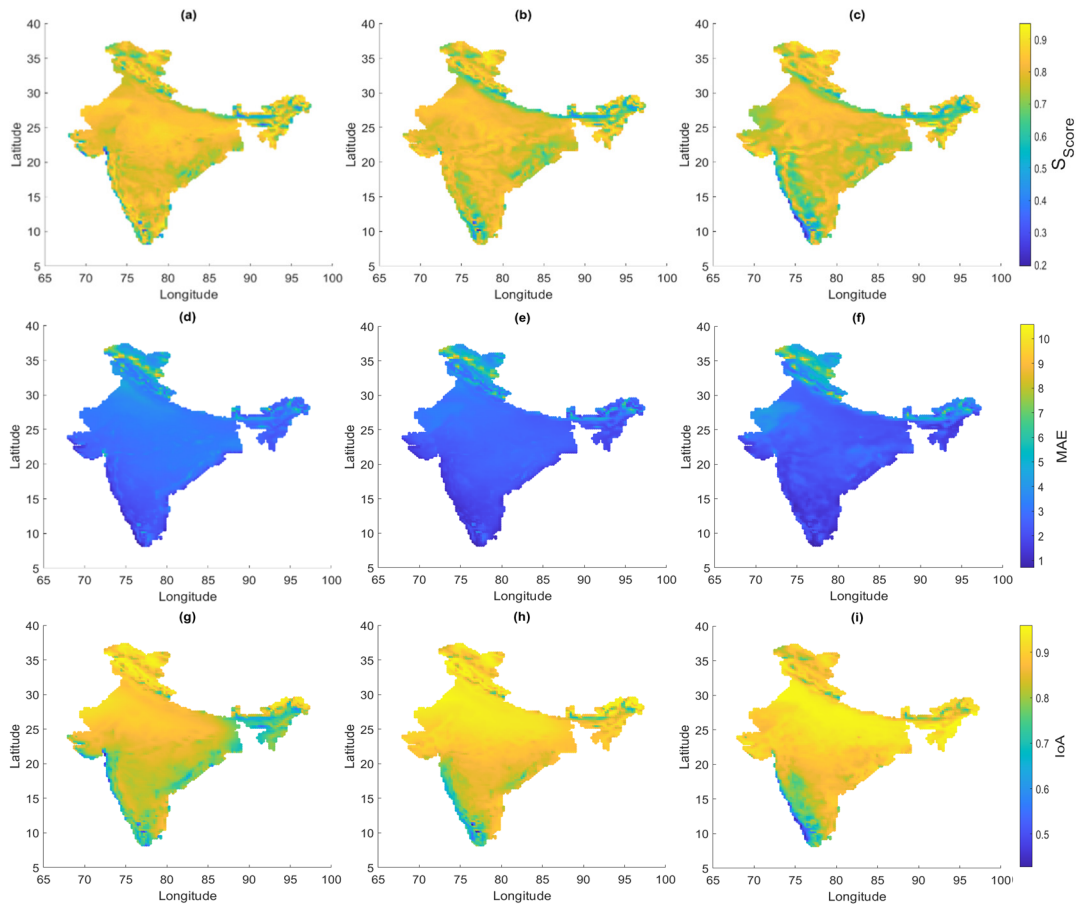


Fig. 7. Values of  $S_{Score}$  ((a) to (c)),  $MAE$  ((d) to (f)) and  $IoA$  ((g) to (i)) produced by EC-Earth3 of CMIP6 in simulating  $T_{max}$  ((a), (d), (g)),  $T_{mean}$  ((b), (e), (h)) and  $T_{min}$  ((c), (f), (i)) considering whole year's data.

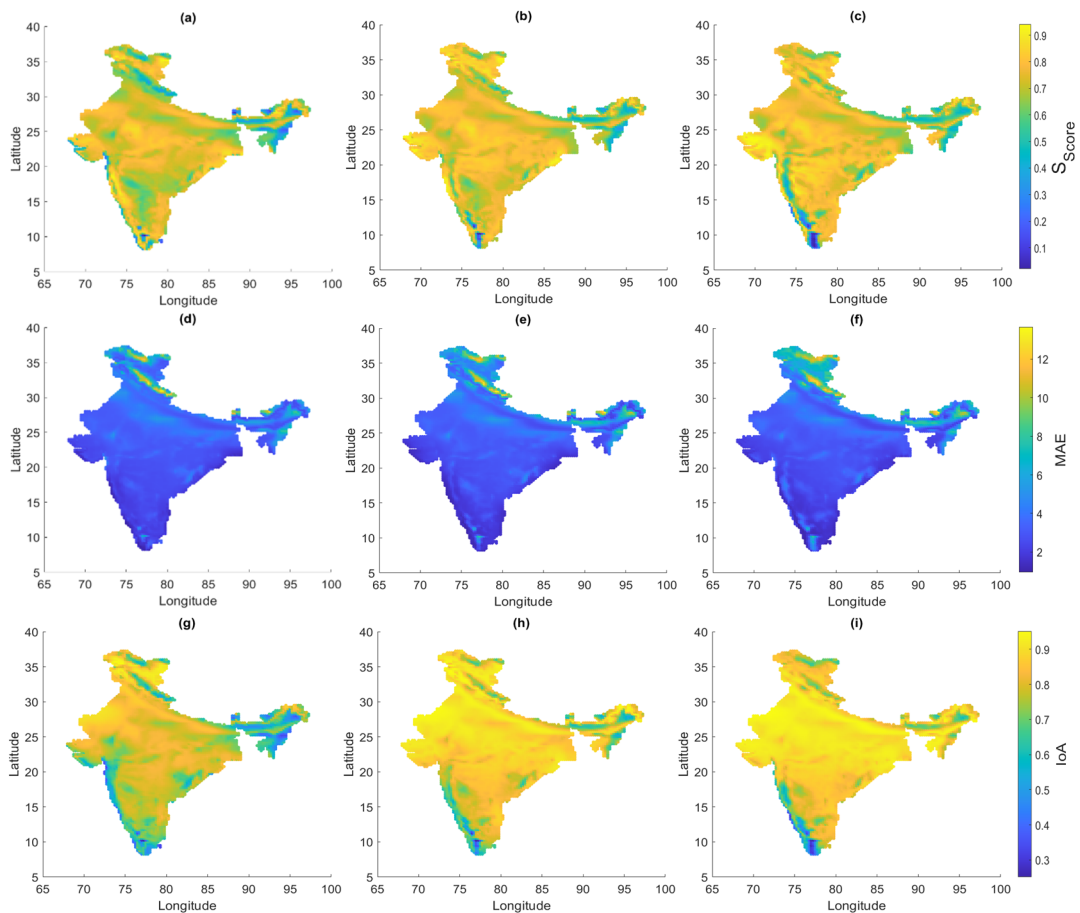


Fig. 8. Values of  $S_{Score}$  ((a) to (c)),  $MAE$  ((d) to (f)) and  $IoA$  ((g) to (i)) produced by CMCC-CMS of CMIP5 in simulating  $T_{max}$  ((a), (d), (g)),  $T_{mean}$  ((b), (e), (h)) and  $T_{min}$  ((c), (f), (i)) considering whole year's data.

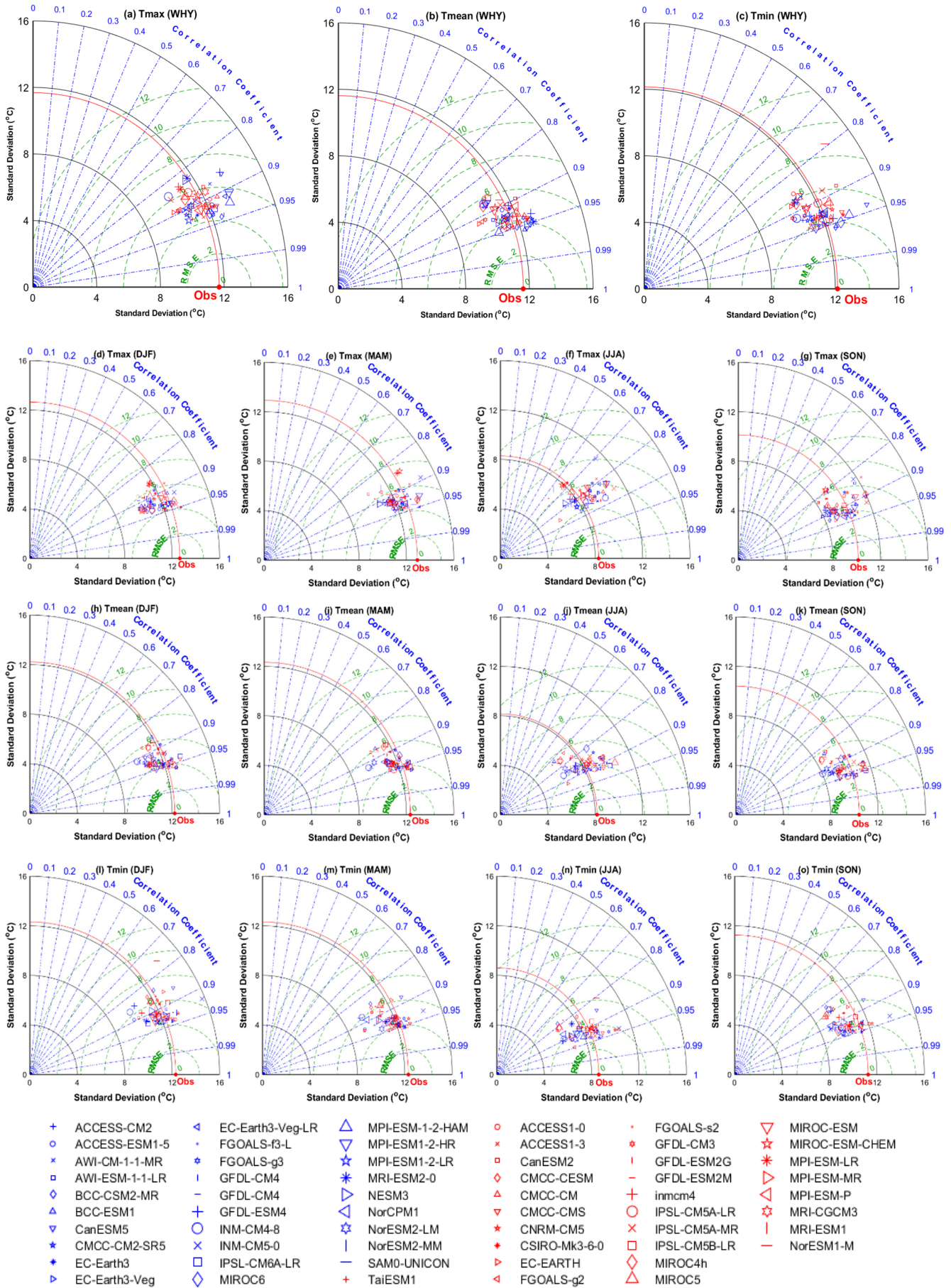


Fig. 9. Taylor diagrams showing the performance of all models of CMIP6 (in blue) and CMIP5 (in red) in simulating  $T_{max}$ ,  $T_{mean}$  and  $T_{min}$  by considering data of whole year (WHY) and four seasons (JJA, SON, DJF, MAM).

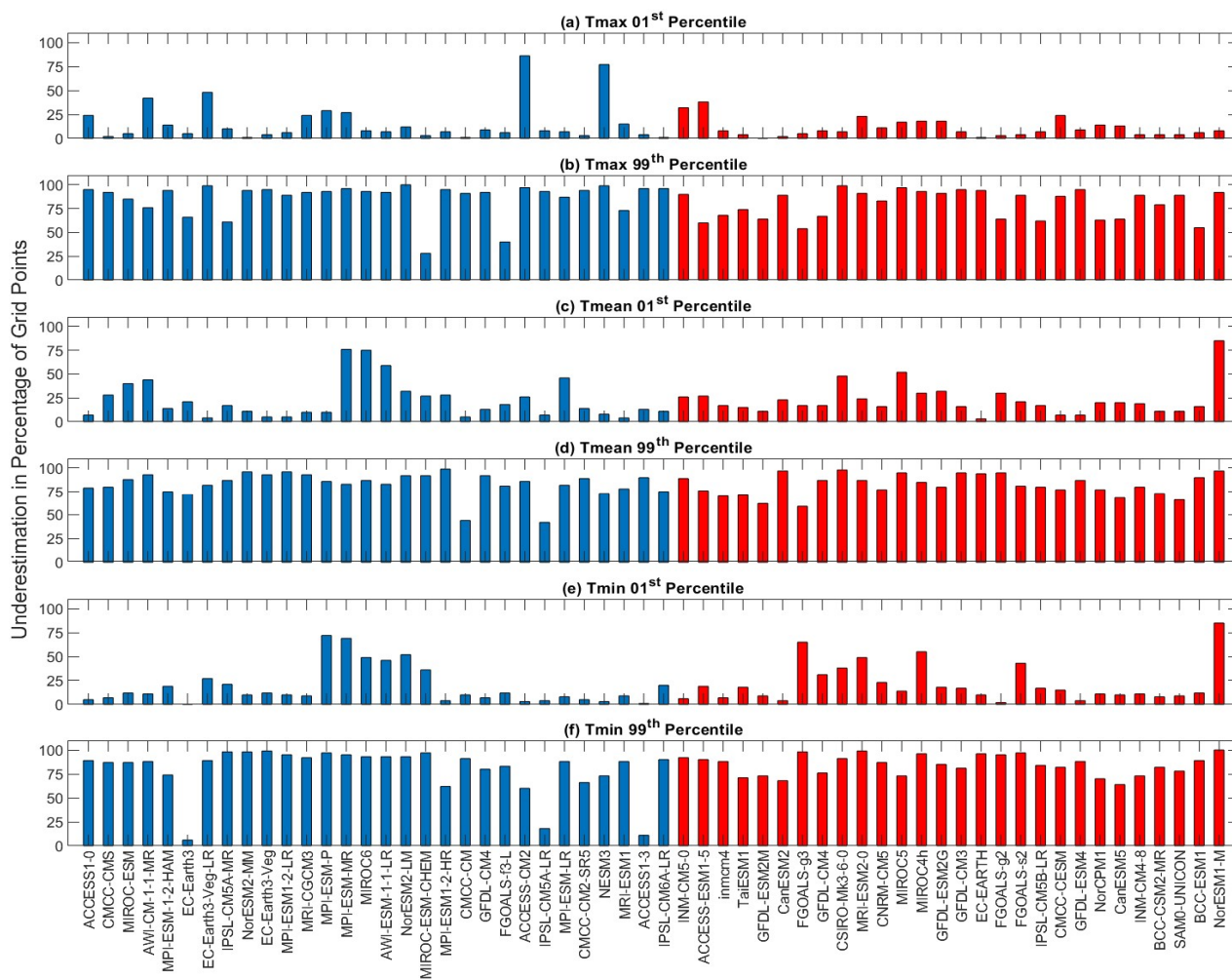


Fig. 10. Percentage of grid-points in which the 1<sup>st</sup> and 99<sup>th</sup> percentiles of  $T_{max}$ ,  $T_{mean}$  and  $T_{min}$  are underestimated by all selected GCMs of CMIP6 (in blue) and CMIP5 (in red).

In order to further explore the simulation performance of the temperature extremes over mainland India, the over- or under-estimation of the 1<sup>st</sup> and 99<sup>th</sup> percentiles were estimated at each grid-point for each of  $T_{max}$ ,  $T_{mean}$  and  $T_{min}$  by the best model of each of the two CMIP phases as described in subsection B. For this purpose, the over- or under-estimation, i.e., error, of a temperature extreme by a GCM was calculated as the deviation of a selected percentile of the model-estimated data computed over the whole data period from that of the reference data expressed as percentage of the latter. A positive or a negative value of this percent (%) error indicates an over- or under-estimation of a temperature extreme. Accordingly, the over- or under-estimation of the extreme values by EC-Earth3 of CMIP6 and CMCC-CMS of CMIP5 at all grid points are presented on the maps of India in Fig. 11 and 12 respectively.

It may be found from Fig. 10 that the 1<sup>st</sup> percentile extremes of  $T_{max}$ ,  $T_{mean}$  and  $T_{min}$  are generally overestimated and the 99<sup>th</sup> percentile extremes are generally underestimated in large fractions of the grid points across mainland India by both models. These observations are reflected in Figs. 11 and 12. With reference to Fig. 1, it appears from these two figures that both models produce large underestimations of the 1<sup>st</sup> percentile extremes in the mountainous regions of the north and northeast India and considerably large overestimations in the north and central Indian plains. Parts of south and west India exhibit a relatively small overestimation of the 1<sup>st</sup>

percentile extremes by both models. In the case of the 99<sup>th</sup> percentile extremes, both models yield relatively large underestimations of  $T_{max}$ ,  $T_{mean}$  and  $T_{min}$  in the mountainous regions of the north and northeast India like those in the case of the 1<sup>st</sup> percentile extremes. For the rest of India, relatively small underestimations are produced by EC-Earth3 of CMIP6 and relatively small overestimations are produced by CMCC-CMS of CMIP5 in simulating the 1<sup>st</sup> percentile extremes of  $T_{max}$  and  $T_{mean}$ . For the simulation of  $T_{min}$  by EC-Earth3 model, the degree of underestimation of the 99<sup>th</sup> percentile extremes appear as being pronounced over much of mainland India with considerable underestimations occurring in the mountainous regions of the north and northeast. However, when simulated by CMCC-CMS, the 99<sup>th</sup> percentile extremes appear as being better simulated than EC-Earth3 with relatively small overestimations over much of India and considerable underestimations in the mountainous regions of the north and northeast India and in some patches on the west, south and central India. These discernible patterns of simulations of temperature extremes by the two GCMs appear as being closely related to the broad topographical and climatological features of mainland India. Suitable methods of bias correction with reference to physiographical characteristics may be devised in future studies for reducing errors in estimating temperature extremes by GCMs of either of the two CMIP phases at different locations of mainland India.

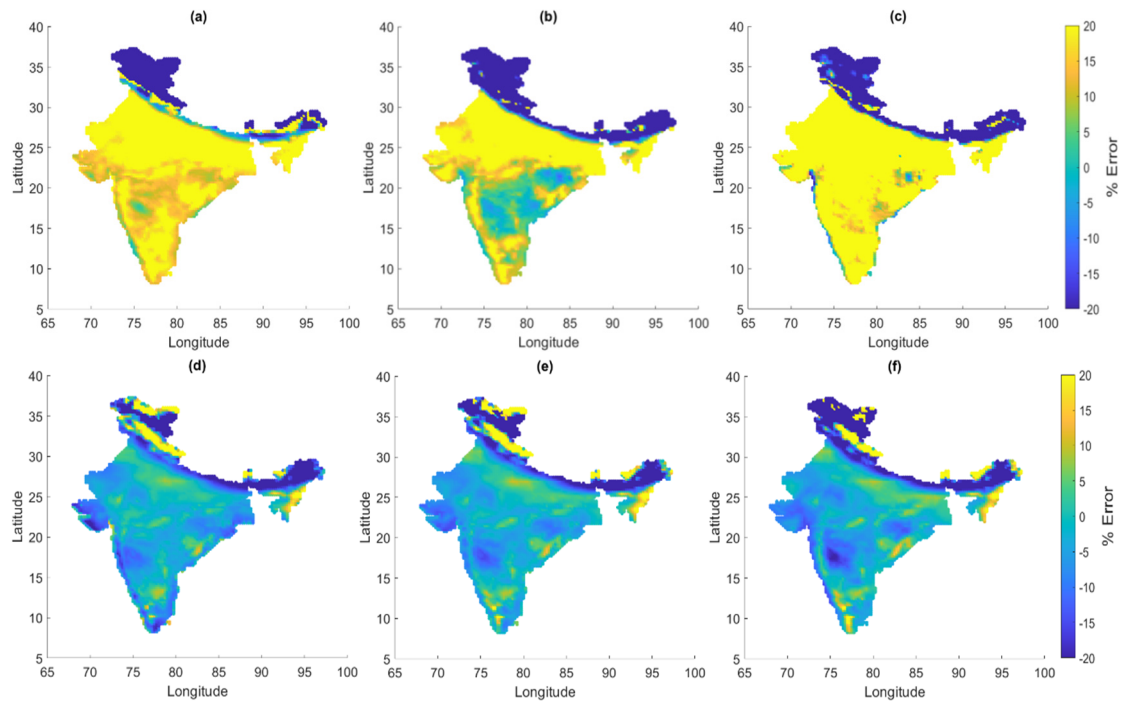


Fig. 11. Spatial distribution of % error (+ve for over- and -ve for under-estimation) of the 1<sup>st</sup> percentile ((a) to (c)) and 99<sup>th</sup> percentile ((d) to (f)) of  $T_{max}$  ((a) and (d)),  $T_{mean}$  ((b) and (e)) and  $T_{min}$  ((c) and (f)) by EC-Earth3 of CMIP6.

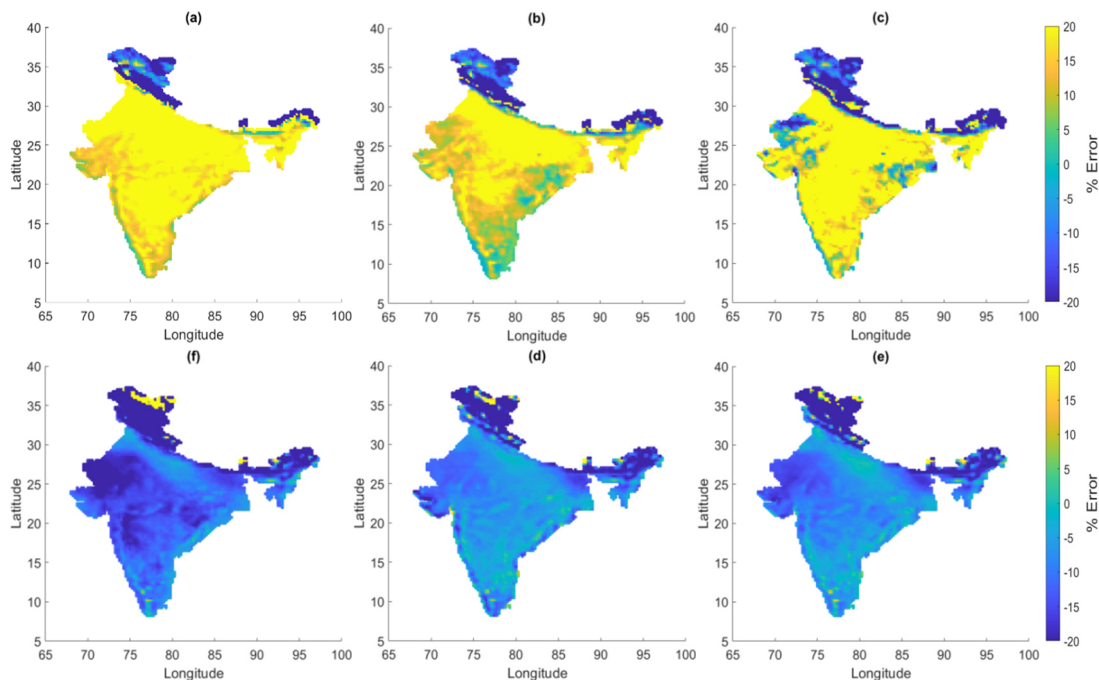


Fig. 12. Spatial distributions of % error (+ve for over- and -ve for under-estimation) of the 1<sup>st</sup> percentile ((a) to (c)) and 99<sup>th</sup> percentile ((d) to (f)) of  $T_{max}$  ((a) and (d)),  $T_{mean}$  ((b) and (e)) and  $T_{min}$  ((c) and (f)) by CMCC-CMS of CMIP5.

## V. CONCLUSIONS AND RECOMMENDATIONS

Several important inferences are drawn based on the performance of 30 GCMs of CMIP6 and 28 of CMIP5 in simulating the maximum ( $T_{max}$ ), mean ( $T_{mean}$ ) and minimum ( $T_{min}$ ) temperature variables and their extremes at 4964 points at  $0.25^\circ \times 0.25^\circ$  grids covering mainland India (excluding the islands).

The spatial distribution of each of CMIP6 and CMIP5 associated with a GCM performing best in simulating each of  $T_{max}$ ,  $T_{mean}$  and  $T_{min}$  at each grid point across India revealed that the GCMs of each phase yielded a larger spatial coverage for one or the other variable over one or the other data-period

(annual or seasonal). It is therefore concluded that, although GCMs of CMIP6 may be expected to perform better than those of the earlier phases of development, the GCMs of CMIP5 still have value in reproducing the maximum, mean and minimum temperature at locations across mainland India. Further, the pattern of spatial distribution of the two CMIP phases vis-a-vis topography and climatic zones of India, indicates the possibility of correspondence of the performance of the GCMs of each CMIP phase with topographical and climatological features of mainland India, and hence the possibility of devising suitable methods of bias correction by incorporating physiographical characteristics for reducing errors in estimating each of  $T_{max}$ ,  $T_{mean}$  and  $T_{min}$  at

different locations of mainland India by GCMs of either of the two CMIP phases.

From the consideration of spatial averaging, the attainment of the best ranks by two GCMs of CMIP6 in individually simulating  $T_{max}$  and  $T_{mean}$  and one GCM of CMIP5 in simulating  $T_{min}$  across all grid points over mainland India indicates that models of CMIP5 would be reliable in simulating and projecting future values of  $T_{min}$ . The results of aggregating the ranks of each model yielding two models of CMIP6 as being the best and second-best, and one model of CMIP5 as being the third best with the ranks of the second- and third-best models being close also indicates that CMIP5 has value comparable to that of CMIP6.

The pattern of the performance of the best model of each CMIP phase, i.e. EC-Earth3 of CMIP6 and CMCC-CMS from CMIP5, identified from aggregation of ranks of all models in simulating  $T_{max}$ ,  $T_{mean}$  and  $T_{min}$  also implies that the best model of either of the two CMIP phases would be applicable for simulating historical data of temperature and projecting future impacts of climate change at any location, particularly at non-grid-points of India for which location-specific studies of climate models may not be feasible for identifying a suitable GCM.

The visual assessment of spatial similarity of the GCMs of the both phases from Taylor diagrams show absence of any distinct clustering of models of different CMIP phases or a large scatter of the models, thereby indicating that the statistical characteristics of the GCMs of both CMIP6 and CMIP5 are comparable and that CMIP5 models also have value in producing reliable estimates of  $T_{max}$ ,  $T_{mean}$  and  $T_{min}$  in simulation and, hence, in future projections.

In respect of temperature extremes, large fractions of grid-points over mainland India are found to be characterized by overestimation of the 1<sup>st</sup> percentile and underestimation of

the 99<sup>th</sup> percentile of each of the three temperature variables. However, no distinct pattern is found to suggest the superiority of one phase on the other in simulating these two extremes. From the grid-point level simulation of model performance by the best model of each CMIP phase identified from the aggregation of ranks, i.e., EC-Earth3 of CMIP6 and CMCC-CMS of CMIP5, it is concluded that the performance of the models of both CMIP phases in simulating the 1<sup>st</sup> and 99<sup>th</sup> percentiles are comparable, and that some correspondence of the pattern of model performance with topographical and climatological features is likely.

In essence, it is concluded that, being developed in the latest phase, models of CMIP6 expectedly perform better in several cases of simulating  $T_{max}$ ,  $T_{mean}$ ,  $T_{min}$  and temperature extremes over mainland India. However, models of CMIP5 also perform either better than or at par with those of CMIP6 in some cases. The results of this study clearly indicate that CMIP5 models still have value in simulating temperature, and, hence, in projecting future impacts under different climate change scenarios based on their geographic disposition, and the temperature statistic and the annual or seasonal data considered, and, hence, in future projections of climate impacts at locations across mainland India based on their geographic disposition, and the temperature statistic and the annual or seasonal data considered. The results of this study also indicate the possibility of suitably incorporating extraneous parameters related to physiographical dispositions of a location for devising efficient methods of bias correction in future research towards improving performance of climate models in simulating different temperature variables.

APPENDIX

Table A1. Details of the selected GCMs of CMIP5

Sl. No.	Model name	Resolution (Long × Lat)	Institution
1	MIROC4h	640×320	AORI (Atmosphere and Ocean Research Institute), NIES (National Institute for Environmental Studies), JAMSTEC (Japan Agency for Marine-Earth Science and Technology), Japan
2	ACCESS1-0	192×145	Commonwealth Scientific and Industrial Research Organisation and Bureau of Meteorology, Australia
3	ACCESS1-3	192×145	
4	CMCC-CESM	96×48	
5	CMCC-CMS	192×96	Centro Euro-Mediterraneo per i Cambiamenti, Italy
6	CMCC-CM	480×240	
7	CNRM-CM5	256×128	Centre National de Recherches Meteorologiques, Meteo-France, France
8	CSIRO-Mk3-6-0	192×96	Australian Commonwealth Scientific and Industrial Research Organization, Australia
9	CanESM2	128×64	Canadian Centre for Climate Modelling and Analysis, Canada
10	EC-EARTH	320×160	EC-Earth (European Earth System Model)
11	FGOALS-g2	128×60	Institute of Atmospheric Physics, Chinese Academy of Sciences, China
12	FGOALS-s2	128×108	
13	GFDL-CM3	144×90	Geophysical Fluid Dynamics Laboratory, USA
14	GFDL-ESM2G	144×90	
15	GFDL-ESM2M	144×90	
16	IPSL-CM5A-LR	96×96	Institut Pierre-Simon Laplace, France
17	IPSL-CM5A-MR	144×143	
18	IPSL-CM5B-LR	96×96	
19	MIROC-ESM-CHEM	128×64	AORI (Atmosphere and Ocean Research Institute), NIES (National Institute for Environmental Studies), JAMSTEC (Japan Agency for Marine-Earth Science and Technology), Japan
20	MIROC-ESM	128×64	
21	MIROC5	256×128	
22	MPI-ESM-LR	192×96	Max Planck Institute for Meteorology, Germany

Sl. No.	Model name	Resolution (Long × Lat)	Institution
23	MPI-ESM-MR	192×96	Meteorological Research Institute, Japan
24	MPI-ESM-P	192×96	
25	MRI-CGCM3	320×160	
26	MRI-ESM1	320×160	
27	NorESM1-M	144×96	Norwegian Climate Centre, Norway
28	inmcm4	180×120	Institute for Numerical Mathematics, Russia

Table A2. Details of the selected GCMs of CMIP6

Sl. No.	Model name	Resolution (Long × Lat)	Institution
1	ACCESS-CM2	192×144	Commonwealth Scientific and Industrial Research Organisation and Australian Research Council Centre of Excellence for Climate System Science, Australia
2	ACCESS-ESM1-5	192×145	
3	AWI-CM-1-1-MR	384×192	Alfred Wegener Institute, Helmholtz Centre for Polar and Marine Research, Bremerhaven, Germany
4	BCC-CSM2-MR	320×160	Beijing Climate Center, China Meteorological Administration, China
5	BCC-ESM1	128×64	
6	CMCC-CM2-SR5	288×192	Fondazione Centro Euro-Mediterraneo sui Cambiamenti Climatici, Italy
7	CanESM5	128×64	Canadian Centre for Climate Modelling and Analysis, Canada
8	EC-Earth3-Veg-LR	512×256	EC-Earth-Consortium
9	EC-Earth3-Veg-LR	320×160	
10	EC-Earth3	512×256	
11	FGOALS-f3-L	288×180	Chines Academy of Sciences, China
12	FGOALS-g3	180×80	
13	GFDL-CM4_gr1	360×180	Geophysical Fluid Dynamics Laboratory, USA
14	GFDL-CM4_gr2	144×96	
15	GFDL-ESM4	288×180	
16	INM-CM4-8	180×120	Institute for Numerical Mathematics, Russia
17	INM-CM5-0	180×120	
18	IPSL-CM6A-LR	144×143	Institut Pierre-Simon Laplace, France
19	MIROC6	256×128	JAMSTEC, AORI, NIES, R-CCS, Japan
20	MPI-ESM-1-2-HAM	192×96	HAMMOZ-Consortium
21	MPI-ESM1-2-HR	384×192	Max Planck Institute for Meteorology, Germany
22	MPI-ESM1-2-LR	192×96	
23	MRI-ESM2-0	320×160	Meteorological Research Institute, Japan
24	NESM3	192×96	Nanjing University of Information Science and Technology, China
25	NorCMP1	144×96	NorESM climate modeling Consortium of CICERO, MET-Norway, NERSC, NILU, UiB, UiO and UNI, Norway
26	NorESM2-LM	144×96	
27	NorESM2-MM	288×192	
28	SAM0-UNICON	288×192	Seoul National University, Korea
29	TaiESM1	288×192	Research Center for Environmental Changes, Academia Sinica, Taiwan
30	AWI-CM-1-1-LR	192×96	Alfred Wegener Institute, Helmholtz Centre for Polar and Marine Research, Bremerhaven, Germany

#### CONFLICT OF INTEREST

The authors declare no conflict of interest.

#### AUTHOR CONTRIBUTIONS

A.P. conceptualized, carried out detailed numerical analyses, and prepared graphical outputs of the study. M.G. suggested improvements on a few aspects of analysis, and prepared the manuscript.

#### DATA AVAILABILITY STATEMENT

GCM outputs of CMIP5 is available at <https://esgf-node.llnl.gov/projects/cmip5/> and of CMIP6 is available at <https://esgf-node.llnl.gov/projects/cmip6/>

#### REFERENCES

- [1] J. Hay and N. Mimura, “The changing nature of extreme weather and climate events: Risks to sustainable development,” *Geomatics, Natural Hazards and Risk*, 2010, vol. 1, pp. 3–18. doi: 10.1080/19475701003643433
- [2] R. A. Bradstock, K. A. Hammill, L. Collins, and O. Price, “Effects of weather, fuel and terrain on fire severity in topographically diverse landscapes of South-Eastern Australia,” *Landscape Ecol.*, 2010, vol. 25, pp. 607–619. doi: 10.1007/s10980-009-9443-8
- [3] S. Shahid, “Probable impacts of climate change on public health in Bangladesh,” *Asia Pac J Public Health* 2010, vol. 22, pp. 310–319. doi: 10.1177/1010539509335499
- [4] B. Zheng, K. Chenu, M. Dreccer, and S. C. Chapman, “Breeding for the future: What are the potential impacts of future frost and heat events on sowing and flowering time requirements for Australian bread wheat (*Triticum Aestivum*) varieties?” *Glob Change Biol.*, 2012, vol. 18, pp. 2899–2914. doi: 10.1111/j.1365-2486.2012.02724.x
- [5] Y. Hirabayashi, R. Mahendran, S. Koirala, L. Konoshima, D. Yamazaki, S. Watanabe, H. Kim, S. Kanae, “Global flood risk under climate change,” *Nature Clim Change*, 2013, vol. 3, pp. 816–821. doi: 10.1038/nclimate1911
- [6] A. AghaKouchak, L. Cheng, O. Mazdiyasi, and A. Farahmand, “Global warming and changes in risk of concurrent climate extremes: Insights from the 2014 California drought: Global warming and concurrent extremes,” *Geophys. Res. Lett.*, 2014, vol. 41, pp. 8847–8852. doi: 10.1002/2014GL062308
- [7] C. Rosenzweig, J. Elliott, D. Deryng, A. C. Ruane *et al.*, “Assessing agricultural risks of climate change in the 21st century in a global

- gridded crop model intercomparison,” in *Proc. Natl. Acad. Sci.*, 2014, vol. 111, pp. 3268–3273. doi: 10.1073/pnas.1222463110
- [8] J. Schewe, J. Heinke *et al.*, “Multimodal assessment of water scarcity under climate change,” in *Proc Natl Acad Sci.*, 2014, vol. 111, pp. 3245–3250. doi: 10.1073/pnas.1222460110
- [9] A. G. Yilmaz, I. Hossain, and B. J. C. Perera, “Effect of climate change and variability on extreme rainfall intensity–frequency–duration relationships: A case study of Melbourne,” *Hydrol. Earth Syst. Sci.*, 2014, vol. 18, pp. 4065–4076. doi: 10.5194/hess-18-4065-2014
- [10] J. Nairn and R. Fawcett, “The excess heat factor: A metric for heatwave intensity and its use in classifying heatwave severity,” *IJERPH* 2014, vol. 12, pp. 227–253. doi:10.3390/ijerph120100227
- [11] S. Whitmee *et al.*, “Safeguarding human health in the anthropocene epoch: report of the rockefeller foundation-lancet commission on planetary health,” *Lancet*, 2015, vol. 386, pp. 1973–2028. doi: 10.1016/S0140-6736(15)60901-1
- [12] M. T. H. Vliet, L. P. H. Beek, S. Eisner, M. Flörke, Y. Wada, and M. F. P. Bierkens, “Multi-model assessment of global hydropower and cooling water discharge potential under climate change,” *Global Environmental Change*, 2016, vol. 40, pp. 156–170. doi: 10.1016/j.gloenvcha.2016.07.007
- [13] J. Huang, H. Yu, A. Dai, Y. Wei, and L. Kang, “Drylands face potential threat under 2 °C global warming target,” *Nature Clim Change*, 2017, vol. 7, pp. 417–422 doi: 10.1038/nclimate3275
- [14] G. T. Pecl *et al.*, “Biodiversity redistribution under climate change: impacts on ecosystems and human well-being,” *Science*, 2017, vol. 355, eaai9214. doi: 10.1126/science.aai9214
- [15] N. Nishant, G. Virgilio, F. Ji, E. Tam, K. Beyer, and M. L. Riley, “Evaluation of present-day CMIP6 model simulations of extreme precipitation and temperature over the Australian continent,” *Atmosphere*, 2022, vol. 13, p. 1478. doi: 10.3390/atmos13091478
- [16] N. H. Stern, *The Economics of Climate Change: The Stern Review*, Cambridge University Press: Cambridge, 2006, ISBN 978-0-521-70080-1.
- [17] OECD: Organisation for Economic Co-operation and Development, *OECD Economic Outlook: Preliminary Version*, OECD Economic Outlook, OECD, 2023, vol. 2023 (1), ISBN 978-92-64-85354-6.
- [18] C. S. Rao, R. S. Prasad, and T. Mohapatra, *Climate Change and Indian Agriculture: Impacts, Coping Strategies, Programmes and Policy*, Indian Council of Agricultural Research, Ministry of Agriculture and Farmers’ Welfare and Ministry of Environment, Forestry and Climate Change, Government of India: New Delhi, India, 2019, p. 26.
- [19] WCRP: World Climate Research Programme WCRP Coupled Model Intercomparison Project (CMIP). [Online]. Available: <https://www.wcrp-climate.org/wgcm-cmip>
- [20] V. Eyring, S. Bony, G. A. Meehl, C. A. Senior, B. Stevens, R. J. Stouffer, and K. E. Taylor, “Overview of the Coupled Model Intercomparison Project Phase 6 (CMIP6) experimental design and organization,” *Geoscientific Model Development*, 2016, vol. 9, pp. 1937–1958. doi: 10.5194/gmd-9-1937-2016.
- [21] WCRP: World Climate Research Programme CMIP6 Source id Values [Online]. Available: [https://wcrp-cmip.github.io/CMIP6\\_CVs/docs/CMIP6\\_source\\_id.html](https://wcrp-cmip.github.io/CMIP6_CVs/docs/CMIP6_source_id.html)
- [22] M. Stockhause, R. Matthews, A. Pirani, A. M. Treguier, and O. Yelekci, *CMIP6 Data Documentation and Citation in IPCC’s Sixth Assessment Report (AR6)*, Copernicus Meetings, 2021;
- [23] IPCC (Intergovernmental Panel on Climate Change), *Climate Change 2023: AR6 Synthesis Report*, Longer Report 2023.
- [24] K. E. Taylor, R. J. Stouffer, and G. A. Meehl, “An overview of CMIP5 and the experiment design,” *Bulletin of the American Meteorological Society*, 2012, vol. 93, pp. 485–498. doi: 10.1175/BAMS-D-11-00094.1
- [25] IPCC (Intergovernmental Panel on Climate Change), *AR5 Synthesis Report: Climate Change 2014 — IPCC*, IPCC, Geneva, Switzerland, 2014, p. 151.
- [26] G. M. Flato, “Earth system models: An overview,” *WIREs Clim Change*, 2011, vol. 2, pp. 783–800. doi:10.1002/wcc.148
- [27] H. Chen, J. Sun, and X. Chen, “Projection and uncertainty analysis of global precipitation-related extremes using CMIP5 models,” *International Journal of Climatology*, 2014, vol. 34, pp. 2730–2748, doi: 10.1002/joc.3871
- [28] J. Marotzke *et al.*, “Climate research must sharpen its view,” *Nature Clim Change*, 2017, vol. 7, pp. 89–91. doi: 10.1038/nclimate3206
- [29] J. Li, R. Huo, H. Chen, Y. Zhao, and T. Zhao, “Comparative assessment and future prediction using CMIP6 and CMIP5 for annual precipitation and extreme precipitation simulation,” *Front. Earth Sci.*, 2021, vol. 9, 687976. doi:10.3389/feart.2021.687976
- [30] M. Wehner, P. Gleckler, and J. Lee, “Characterization of long period return values of extreme daily temperature and precipitation in the CMIP6 models: Part 1, model evaluation,” *Weather and Climate Extremes*, 2020, 30, 100283. doi: 10.1016/j.wace.2020.100283
- [31] X. Fan, C. Miao, Q. Duan, C. Shen, and Y. Wu, “The performance of cmip6 versus CMIP5 in simulating temperature extremes over the global land surface,” *Journal of Geophysical Research: Atmospheres* 2020, vol. 125, e2020JD033031. doi: 10.1029/2020JD033031
- [32] H. Chen, J. Sun, W. Lin, and H. Xu, “Comparison of CMIP6 and CMIP5 models in simulating climate extremes,” *Science Bulletin*, 2020, vol. 65, pp. 1415–1418. doi: 10.1016/j.scib.2020.05.015
- [33] Y.-H. Kim, S.-K. Min, X. Zhang, J. Sillmann, and M. Sandstad, “Evaluation of the CMIP6 multi-model ensemble for climate extreme indices,” *Weather and Climate Extremes*, 2020, vol. 29, 100269, doi: 10.1016/j.wace.2020.100269
- [34] K. Shashikanth, K. Salvi, S. Ghosh, and K. Rajendran, “Do CMIP5 Simulations of indian summer monsoon rainfall differ from those of CMIP3?: CMIP3 and CMIP5 comparison for Indian monsoon,” *Atmos. Sci. Lett.*, 2014, vol. 15, pp. 79–85. doi: 10.1002/asl2.466
- [35] J. K. Meher, L. Das, J. Akhter, R. E. Benestad, and A. Mezghani, Performance of CMIP3 and CMIP5 GCMs to simulate observed rainfall characteristics over the Western Himalayan Region,” *Journal of Climate*, 2017, vol. 30, pp. 7777–7799. doi: 10.1175/JCLI-D-16-0774.1
- [36] M. Almazroui, S. Saeed, F. Saeed, M. N. Islam, and M. Ismail, “Projections of precipitation and temperature over the South Asian countries in CMIP6,” *Earth Syst Environ.*, 2020, vol. 4, pp. 297–320, doi: 10.1007/s41748-020-00157-7
- [37] P. Kumar and P. P. Sarthi, “Intraseasonal variability of indian summer monsoon rainfall in CMIP6 models simulation,” *Theor Appl Climatol.*, 2021, vol. 145, pp. 687–702. doi: 10.1007/s00704-021-03661-6
- [38] S. Anil and P. Raj, “Deciphering the projected changes in CMIP-6 based precipitation simulations over the Krishna River basin,” *Journal of Water and Climate Change*, 2022, vol. 13, pp. 1389–1407. doi: 10.2166/wcc.2022.399
- [39] K. Rao, T. V. Kumar *et al.*, “Characteristic changes in climate projections over indus basin using the bias corrected CMIP6 simulations,” *Clim Dyn.*, 2022, vol. 58, pp. 3471–3495. doi: 10.1007/s00382-021-06108-w
- [40] M. Guilbert, P. Terray, and J. Mignot, “Intermodel spread of historical indian monsoon rainfall change in CMIP6: The role of the tropical pacific mean state,” *Journal of Climate*, 2023, vol. 36, pp. 3937–3953, doi: 10.1175/JCLI-D-22-0585.1
- [41] K. Raju, P. Sonali, and D. Kumar, “Ranking of CMIP5-based global climate models for india using compromise programming,” *Theoretical and Applied Climatology*, 2016, vol. 128, pp. 563–574, doi: 10.1007/s00704-015-1721-6
- [42] G. Basha *et al.*, “Historical and projected surface temperature over india during the 20th and 21st century,” *Sci Rep*, 2017, vol. 7, p. 2987, doi: 10.1038/s41598-017-02130-3
- [43] C. G. Madhusoodhanan, K. Shashikanth, T. I. Eldho, and S. Ghosh, “Can statistical downscaling improve consensus among CMIP5 models for Indian summer monsoon rainfall projections?” *Int. J. Climatol.*, 2018, vol. 38, pp. 2449–2461. doi: 10.1002/joc.5352
- [44] A. Gusain, S. Ghosh, and S. Karmakar, “Added value of CMIP6 over CMIP5 models in simulating Indian summer monsoon rainfall,” *Atmospheric Research*, 2020, vol. 232, 104680. doi: 10.1016/j.atmosres.2019.104680
- [45] P. Salunke and S. K. Mishra, *Evaluation of Indian Summer Monsoon Precipitation Using CMIP5 and CMIP6 Models*, European Geophysical Union, 2022.
- [46] U. Dutta, A. Hazra, H. S. Chaudhari, S. K. Saha, S. Pokhrel, and U. Verma, *Unraveling the Global Teleconnections of Indian Summer Monsoon Clouds: Expedition from CMIP5 to CMIP6*, 2021, doi: 10.48550/ARXIV.2109.07122
- [47] P. P. Sreekala, C. A. Babu, and S. V. B. Rao, “On the simulation of Northeast monsoon rainfall over southern peninsular India in CMIP5 and CMIP6 models,” *Theor Appl Climatol.*, 2022, vol. 150, pp. 969–986. doi: 10.1007/s00704-022-04194-2
- [48] A. Katzenberger, J. Schewe, J. Pongratz, and A. Levermann, “Robust increase of Indian monsoon rainfall and its variability under future warming in CMIP6 models,” *Earth Syst. Dynam.*, 2021, vol. 12, pp. 367–386. doi: 10.5194/esd-12-367-2021
- [49] India Meteorological Department Gridded Data Archive. [Online]. Available: <https://www.imdpune.gov.in/lrfindex.php>
- [50] National Center for Atmospheric Research (NCAR), the USA Climate Data Guide (CDG). [Online]. Available: <https://climatedataguide.ucar.edu/climate-data/reanalysis>
- [51] S. S. Mahto and V. Mishra, “Does ERA-5 outperform other reanalysis products for hydrologic applications in India?” *J. Geophys. Res. Atmos.*, 2019, vol. 124, pp. 9423–9441. doi: 10.1029/2019JD031155

- [52] S. E. Perkins, A. J. Pitman, N. J. Holbrook, and J. McAneney, "Evaluation of the AR4 climate models' simulated daily maximum temperature, minimum temperature, and precipitation over Australia using probability density functions," *Journal of Climate*, 2007, vol. 20, pp. 4356–4376. doi: 10.1175/JCLI4253.1
- [53] C. C. Maxino, B. J. McAvaney, A. J. Pitman, and S. E. Perkins, "Ranking the AR4 climate models over the murray-darling basin using simulated maximum temperature, minimum temperature and precipitation," *Int. J. Climatol.*, 2008, vol. 28, pp. 1097–1112. doi: 10.1002/joc.1612
- [54] I. G. Watterson, "Calculation of probability density functions for temperature and precipitation change under global warming," *J. Geophys. Res.*, 2008, vol. 113, D12106. doi: 10.1029/2007JD009254
- [55] G. Fu *et al.*, "A score-based method for assessing the performance of GCMs: A case study of Southeastern Australia: ASSESSING GCMs," *J. Geophys. Res. Atmos.*, 2013, vol. 118, pp. 4154–4167. doi: 10.1002/jgrd.50269
- [56] A. Anandhi and R. S. Nanjundiah, "Performance evaluation of AR4 climate models in simulating daily precipitation over the Indian region using skill scores," *Theor Appl Climatol*, 2015, vol. 119, pp. 551–566. doi: 10.1007/s00704-013-1043-5
- [57] A. G. Koutroulis, M. G. Grillakis, I. K. Tsanis, and L. Papadimitriou, "Evaluation of precipitation and temperature simulation performance of the CMIP3 and CMIP5 historical experiments," *Clim Dyn*, 2015, vol. 47, pp. 1881–1898. doi: 10.1007/s00382-015-2938-x
- [58] Y. Lun, L. Liu, L. Cheng, X. Li, H. Li, and Z. Xu, "Assessment of GCMs simulation performance for precipitation and temperature from CMIP5 to CMIP6 over the Tibetan Plateau," *International Journal of Climatology*, 2021, vol. 41, pp. 3994–4018. doi:10.1002/joc.7055
- [59] N. N. Ridder, A. J. Pitman, and A. M. Ukkola, "Do CMIP6 climate models simulate global or regional compound events skillfully?" *Geophysical Research Letters*, 2021, vol. 48. doi: 10.1029/2020GL091152
- [60] C. J. Willmott, "on the validation of models," *Physical Geography*, 1981, vol. 2, pp. 184–194. doi: 10.1080/02723646.1981.10642213
- [61] C. J. Willmott, S. G. Ackleson, R. E. Davis, J. J. Feddema, K. M. Klink, D. R. Legates, J. O'Donnell, and C. M. Rowe, "Statistics for the evaluation and comparison of models," *J. Geophys. Res.*, 1985, vol. 90, p. 8995. doi: 10.1029/JC090iC05p08995
- [62] Y. H. Song, E.-S. Chung, and S. Shahid, "Spatiotemporal differences and uncertainties in projections of precipitation and temperature in South Korea from CMIP6 and CMIP5 general circulation models," *International Journal of Climatology*, 2021, vol. 41, pp. 5899–5919. doi: 10.1002/joc.7159
- [63] M. Yasin *et al.*, "Climate change impact uncertainty assessment and adaptations for sustainable maize production using multi-crop and climate models," *Environ Sci Pollut Res.*, 2022, vol. 29, pp. 18967–18988. doi: 10.1007/s11356-021-17050-z
- [64] Q. Saddique *et al.*, "Modelling future climate change impacts on winter wheat yield and water use: A case study in Guanzhong Plain, Northwestern China," *European Journal of Agronomy*, 2020, vol. 119, 126113. doi: 10.1016/j.eja.2020.126113
- [65] N. Zhu, J. Xu, C. Wang, Z. Chen, and Y. Luo, "Modeling the multiple time scale response of hydrological drought to climate change in the data-scarce inland river basin of Northwest China," *Arab J Geosci.*, 2019, vol. 12, p. 225. doi: 10.1007/s12517-019-4404-2
- [66] K. E. Taylor, "Summarizing multiple aspects of model performance in a single diagram," *J. Geophys. Res.*, 2001, vol. 106, pp. 7183–7192. doi: 10.1029/2000JD900719
- [67] G. Tegegne, A. M. Melesse, and A. W. Worqlul, "Development of multi-model ensemble approach for enhanced assessment of impacts of climate change on climate extremes," *Science of The Total Environment*, 2020, vol. 704, 135357. doi: 10.1016/j.scitotenv.2019.135357
- [68] Y. Zamani, S. A. Monfared, M. Azhdari, and M. Hamidianpour, "A comparison of CMIP6 and CMIP5 projections for precipitation to observational data: The case of Northeastern Iran," *Theor Appl Climatol*, 2020, vol. 142, pp. 1613–1623. doi: 10.1007/s00704-020-03406-x.
- [69] B. Ayugi, J. Zhihong *et al.*, "Comparison of CMIP6 and CMIP5 models in simulating mean and extreme precipitation over East Africa," *International Journal of Climatology*, 2021, vol. 41, pp. 6474–6496. doi: 10.1002/joc.7207
- [70] C.-A. Chen, H.-H. Hsu, and H.-C. Liang, "Evaluation and comparison of CMIP6 and CMIP5 model performance in simulating the seasonal extreme precipitation in the Western North Pacific and East Asia," *Weather and Climate Extremes*, 2021, vol. 31, 100303. doi: 10.1016/j.wace.2021.100303
- [71] N. Luo, Y. Guo, J. Chou, and Z. Gao, "Added value of CMIP6 models over CMIP5 models in simulating the climatological precipitation extremes in China," *International Journal of Climatology*, 2022, vol. 42, pp. 1148–1164. doi: 10.1002/joc.7294
- [72] X. Zhu, S.-Y. Lee *et al.*, "Extreme climate changes over three major river basins in China as seen in CMIP5 and CMIP6," *Clim Dyn*, 2021, vol. 57, pp. 1187–1205. doi: 10.1007/s00382-021-05767-z
- [73] Y. Guo *et al.*, "A comparative assessment of CMIP5 and CMIP6 in hydrological responses of the Yellow River Basin, China," *Hydrology Research*, 2022, vol. 53, pp. 867–891. doi: 10.2166/nh.2022.001
- [74] M. M. Hamed *et al.*, "Inconsistency in historical simulations and future projections of temperature and rainfall: A comparison of CMIP5 and CMIP6 models over Southeast Asia," *Atmospheric Research*, 2022, vol. 265, 105927. doi: 10.1016/j.atmosres.2021.105927
- [75] Y. Yang, Y. Zhang, Z. Gao, Z. Pan, and X. Zhang, "Historical and projected changes in temperature extremes Over China and the inconsistency between multimodel ensembles and individual models from CMIP5 and CMIP6," *Earth and Space Science*, 2023, vol. 10. doi: 10.1029/2022EA002514
- [76] BIS (Bureau of Indian Standards), *National Building Code of India, 2016*, BIS (Bureau of Indian Standards): New Delhi, India, 2016, vol. 2.
- [77] Central Water Commission (CWC), *Flood Estimation Report for Lower Narmada and Tapi Subzone - 3(b) (Revised)*, Central Waater Commission, Government of India, 2004.
- [78] R. Jha and V. Smakhtin, *A Review of Methods of Hydrological Estimation at Ungauged Sites in India*, 2008.
- [79] H. Hersbach *et al.*, *ERA5 Hourly Data on Single Levels from 1940 to Present*, 2023.
- [80] U. Schulzweida, *CDO User Guide*, 2022. doi: 10.5281/ZENODO.7112925

Copyright © 2024 by the authors. This is an open access article distributed under the Creative Commons Attribution License which permits unrestricted use, distribution, and reproduction in any medium, provided the original work is properly cited ([CC BY 4.0](https://creativecommons.org/licenses/by/4.0/)).